# A passively-fed methanol steam reformer heated with two-stage bi-fueled catalytic combustor

Kai-Fan Lo, Shwin-Chung Wong[*]

Department of Power Mechanical Engineering, National Tsing Hua University, Hsin-Chu 300, Taiwan, ROC

## ABSTRACT

This paper presents further progress on our simple novel passively-fed methanol steam reformer. The present study focuses on the development of a catalytic combustor workable with both hydrogen and methanol fuels. The aim is to reutilize the exhaust hydrogen from a fuel cell under stable operation but burn methanol during the start-up. On a copper plate, the catalytic combustor in a u-turn channel is integrally machined under a two-turn serpentine-channel reformer. To resolve the highly different fuel reactivities, a suitably diluted catalyst formula demonstrates uniform temperature distributions burning with either liquid methanol or an $H_2/CO_2$ mixture simulating the exhaust gas from a fuel cell. In a two-stage process, it first takes 25 min to reach 270 °C by burning methanol. After the fuel is switched to the $H_2/CO_2$ mixture, another 20 min is needed to attain an optimal steady state which yields a high methanol conversion of 95% and acceptably low CO fraction of 1.04% at a reaction temperature of 278 °C. The $H_2$ and $CO_2$ concentrations are 75.1% and 23.6%.

© 2012 Elsevier B.V. All rights reserved.

## 1. Introduction

The practical application of hydrogen in PEM fuel cells has been limited by the problems associated with safety and handling of hydrogen. Reforming liquid hydrocarbons provides safe and movable onboard generation of hydrogen. Methanol is an outstanding liquid fuel for reforming because it has a high hydrogen–carbon ratio without carbon–carbon bonds and a potentially high production capacity. A hydrogen-rich gas can be produced onboard by methanol steam reforming (MSR) using a copper-based catalyst [1–6]:

$$CH_3OH_{(g)} + H_2O_{(g)} \rightarrow 3H_2 + CO_2, \quad \Delta H = +49.4 \text{ kJ mol}^{-1} \quad (1)$$
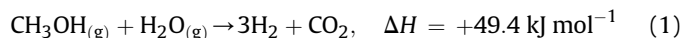
Theoretically, the catalytic steam reforming of methanol yields product gases with a composition of 75% $H_2$ and 25% $CO_2$. Practically, the product gases also contain some residual methanol and a small amount of carbon monoxide (CO), which can be less than 2%. In MSR, reactor performance depends on many factors, such as temperature, pressure, catalyst type, water to methanol ratio, reactor geometry, catalyst particle size, flow pattern, and space velocity [7]. The main advantages of methanol steam reformers (MSRs) are their high hydrogen product concentrations and low

reforming temperatures (200–300 °C) which leads to low CO product concentrations. The main drawbacks of the MSR process are its slow start-up and endothermicity which requires constant heating to maintain reaction temperatures above 250 °C. Consequently, catalytic combustors burning with liquid or gaseous fuels have been developed [8–14].

From the point for energy efficiency, a better way is to reutilize the unconverted hydrogen in the fuel cell exhaust as the fuel of the catalytic combustor. This concept can be seen in some articles [8,11,12,15,16]. However, since the exhaust hydrogen is unavailable during the start-up, an alternative heating source is needed. Another important concern in applications is the uniformity of the heat exchange between the catalytic combustor and the methanol reformer. The presence of cold or hot spots in the reformer will affect the catalyst's lifetime, the conversion efficiency of the reformer, and the CO product concentration [9–11]. Janicke et al. [17] reported a hot spot in the front of the catalytic combustor when a highly combustible $H_2/O_2$ mixture was introduced. Such hot spots should be carefully controlled in order to uniform the temperature distribution of the catalytic combustion of hydrogen for MSR.

In our previous works [14,18], we presented a simple novel passive feeding method for a methanol steam reformer. Using a u-turn-channel methanol-fueled catalytic combustor under the reformer, we achieved highly uniform temperature distributions throughout the reformer and consequently high methanol

## Nomenclature

| | |
|---|---|
| $A$ | cross-sectional area of evaporator |
| $h_{fg}$ | heat of evaporation (kJ mol$^{-1}$) |
| $\dot{m}$ | mass evaporation rate |
| $\dot{m}_{m,c}$ | methanol feed rate to combustor (mol min$^{-1}$) |
| $\dot{m}_{h,c}$ | hydrogen feed rate to combustor (mol min$^{-1}$) |
| $Q$ | heat |
| $R$ | thermal resistance |
| S/C | steam/carbon ratio or water/methanol feed ratio |
| $T$ | temperature (°C); thermocouple |

Subscripts

| | |
|---|---|
| b | boiling point |
| c | combustor |
| h | heater |
| m | methanol |
| r | reaction |
| w | water |

conversions and low CO concentrations [14]. For a fuel cell system including a methanol reformer, methanol can be conveniently used as the combustor fuel during the start-up, while the unconverted hydrogen in the fuel cell exhaust is reutilized during the stable operation. After the reformer reaches a selected reaction temperature, the combustor fuel is switched from methanol to exhaust hydrogen. Therefore, the catalytic combustor must be suitable for both methanol and hydrogen. However, the problem of temperature non-uniformity which tends to occur with hydrogen combustion must be solved. In this paper, we will show that our u-turn channel combustor with a suitable catalyst charge can achieve acceptably uniform temperature distributions for both fuels. Furthermore, in a two-stage bi-fueled operation, the present catalytic combustor renders satisfactory reformer performance in both methanol conversion and CO concentration.

## 2. Experimental

### 2.1. Reformer system

A detailed description of the experimental methods is available in Refs. [14,18]. Here is given a brief introduction including the differences. Fig. 1 illustrates the layout of the present MSR system. The novel, passive thermally-controlled fuel feeding method proposed in Lo and Wong [14,18] is again adopted. A catalytic combustor provides the heat required by the reformer as well as by the vaporization of liquid methanol and water. By selecting the proper thermal resistance of each heat path, a suitable ratio of the fuel vapors can be fed passively to yield stable catalytic reforming reaction. The main difference is that the present system has been modified to allow two different fuels for the catalytic combustor in a two-stage operation. During the start-up stage, liquid methanol from the methanol tank is supplied to the combustor at a fixed feed rate. As soon as the reaction temperature reaches a selected threshold, the combustor fuel is switched using a three-way diverter valve to a hydrogen mixture containing 50% H$_2$ in CO$_2$, which simulates the anode-off exhaust from an MSR-fed fuel cell.

Due to the fixed stoichiometry of the steam reforming reaction, as in Eq. (1), the stoichiometric feed ratio between methanol and water is fixed. In practice, a certain amount of excess water is usually adopted to suppress CO formation. In our design, we dispense the heat flow by managing different thermal resistances, $R_m$ and $R_w$, of the heat paths between the catalytic combustor and
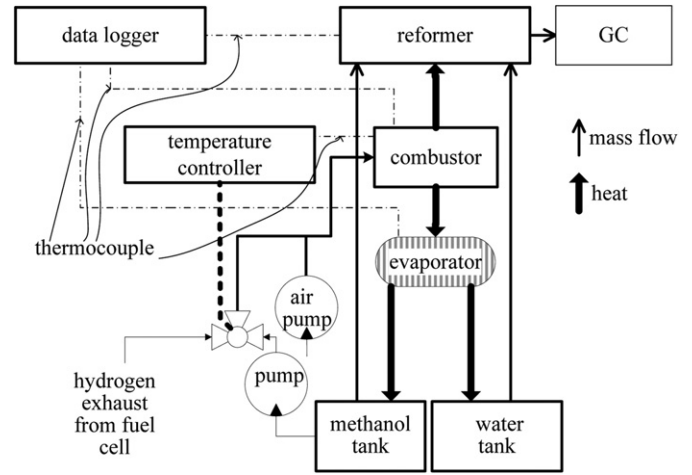


Fig. 1. Present steam reforming system with passive fuel feeding.

the two separate liquid fuel tanks. In the present study, we use the same material and path length but different cross-sectional areas, $A_m$ and $A_w$, to attain different $R_m$ and $R_w$. From a thermal view, different amounts of heat ($q_m$ and $q_w$) are needed by the methanol and the water evaporator because the latent heats of the two fuels are different ($h_{fg,m} = 35.2$ kJ mol$^{-1}$; $h_{fg,w} = 40.63$ kJ mol$^{-1}$).Eqs. (2) and (3) are the related equations:

$$q_m = \frac{T_h - T_{b,m}}{R_m} = \dot{m}_m \times h_{fg,m}, \tag{2}$$

$$q_w = \frac{T_h - T_{b,w}}{R_w} = \dot{m}_w \times h_{fg,w}, \tag{3}$$

where $\dot{m}_m$ and $\dot{m}_w$ are the mass evaporation rates of methanol and water, respectively. The theoretical $q_w/q_m$ ratio is about 1.2 according to Eq. (1) and their latent heats. As for the heat flow $q_r$ needed to sustain the catalytic reaction with $T_r = 250-300$ °C, the proper ratio between $q_r$ and the sum of $q_m$ and $q_w$ can be attained by adjusting $T_h$, which is slightly higher than $T_r$.

### 2.2. The reformer and combustor

Fig. 2 illustrates the detailed arrangement in the unit of the integrated reformer catalyst bed and catalytic combustor. Also shown are the implanted thermocouples, including eight numbered ones, T0–T7, and six unnumbered ones. Thermocouple T0 measures the temperatures at the center of the reformer catalyst bed. The other seven thermocouples, T1–T7, are distributed between the catalyst bed and the combustor to monitor the temperature uniformity. The six unnumbered thermocouples, together with T1 and T2, are used to reflect the detailed temperature distributions along the traveling distance from the combustor inlet. All the thermocouples are K-type and their signals are recorded using a data logger with a resolution of 0.1 K. The length, width and thickness of the integrated unit are 100, 30 and 20 mm, respectively. The copper-based HiFUEL R120 catalyst of Alfa Aesar, in φ5.2 mm × 3.0 mm porous pellets, is used for the MSR reaction. The spacing among the pellets is filled with fine catalyst particles. The length, width and depth of the serpentine channel (cf. Fig. 2a) are 290, 10 and 13 mm, respectively.

With regard to the catalytic combustor, we select a u-turn-channel design (cf. Fig. 2b) that helps achieve uniform temperature distributions in the reforming system. As the exhaust hydrogen and
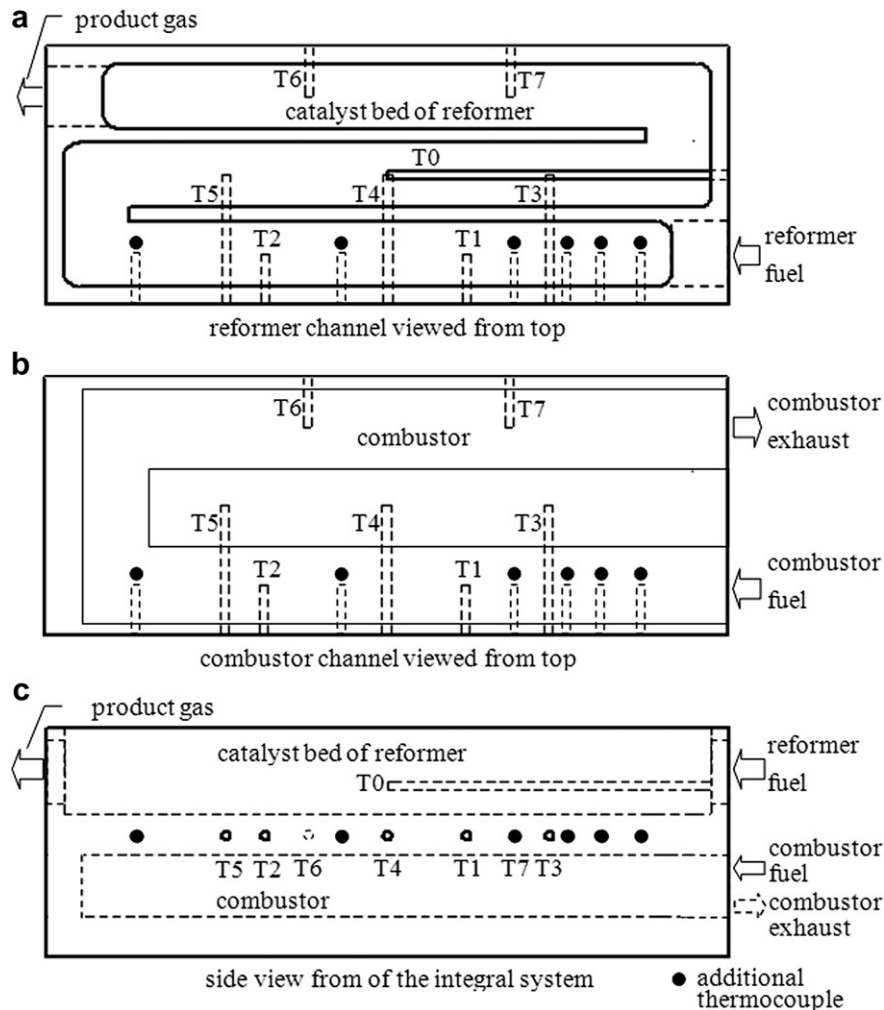
**Fig. 2.** Integrated reformer catalyst bed and catalytic combustor with thermocouple positions.

air are pumped in, combustion is ignited with the highest intensity near the inlet which gradually decays along the traveling distance. With a u-turn channel, the released heat averages between the two parallel counter-flow sections through the copper wall. The u-turn channel has a length of 175 mm and a diameter of 8 mm. In the present work, we adopt two different catalyst formulas. One is the undiluted formula consisting of 6.7 g of 1 mm-diameter JM-AB4 catalyst particles of Johnson Matthey (as in Refs. [14,18]). The other is a diluted formula consisting of 3.65 g JM-AB4 catalyst particles mixed with 4.19 g of 3 mm-diameter alumina particles. The latter is used to attenuate but elongate hydrogen combustion so that temperature uniformity can be improved.

In this study, the area ratio of $A_m/A_w$ is fixed at 0.69. Both fuel tanks are sealed to avoid vapor leakage and the fuels in the tanks are absorbed in capillary wicks. The two kinds of vapors generated from each tank are mixed at the entrance of the reformer catalyst bed. For thermal insulation, the reforming system (including the evaporators) is wrapped with glass fiber plates and put in a Bakelite box, and the vacancy is stuffed with glass fiber cotton.

In our passive feeding method, both S/C and the space velocity vary with the reaction temperature $T_r$, which increases with the feed rate of the combustion fuel. They are not independent parameters as in conventional reforming methods. In the present experiments, the space velocity in the reformer ranges between 4105 h$^{-1}$ and 5061 h$^{-1}$ with methanol combustion and between 3905 h$^{-1}$ and 5175 h$^{-1}$ with hydrogen combustion.

### 2.3. Test conditions

To promote a complete reaction in the catalytic combustor, fuel-lean conditions are made with a fixed air flow rate 0.129 mol min$^{-1}$. The composition of the combustor's exhaust is analyzed using a gas chromatograph (GC, China Chromatography Co.). When the temperature at the middle of the catalyst bed reaches the specified $T_r$, the reaction gradually becomes steady.

Two K-type thermocouples are inserted into each of the evaporators to estimate the heat rates $q_w$ and $q_m$ based on Eqs. (2) and (3). Once they are estimated, the amount of each vapor fuel can be determined. The concentrations of each species in the product gas are determined with the thermal conductivity detector (TCD) of the GC. An amount of 500 μL sample gas is drawn from the product gas and injected into the column (Propark Q, 3 m long). The injector and the column are kept at 120 °C to avoid the condensation of water or methanol. The S/C ratio participating in the reaction can be estimated in two ways. First, it can be calculated from $q_w/q_m$ by

$$S/C = \frac{[H_2O]_{in}}{[MeOH]_{in}} = \left(\frac{q_w}{q_m}\right)\left(\frac{h_{fg,m}}{h_{fg,w}}\right). \tag{4}$$

Or, it can be calculated from the concentrations of the product species. To account for the CO product, we further use the decomposition reaction

$$CH_3OH \rightarrow CO + 2H_2. \tag{5}$$

According to Eqs. (1) and (5),

$$S/C = \frac{[CO_2]_{product} + [H_2O]_{residue}}{[CO_2]_{product} + [CO]_{product} + [MeOH]_{residue}}. \tag{6}$$

The methanol conversion can be estimated by

$$\begin{aligned} Conversion &= \frac{[MeOH]_{in} - [MeOH]_{out}}{[MeOH]_{in}} \\ &= \frac{[CO_2]_{product} + [CO]_{product}}{[CO_2]_{product} + [CO]_{product} + [MeOH]_{residue}}. \end{aligned} \tag{7}$$

By comparing the two S/C ratios respectively from $q_w/q_m$ (Eq. (4)) and the product analysis (Eq. (6)), the reliability of the S/C estimations in the present work can be confirmed.

## 3. Results and discussion

### 3.1. MSR performance with combustion of $H_2$ mixture in undiluted catalyst

The MSR experiments have been first conducted using the undiluted catalyst formula burning with a mixture fuel of 50% $H_2$ and 50% $CO_2$. Depending on the desired $T_r$, the flow rate of the $H_2/CO_2$ mixture, $\dot{m}_{h,c}$, ranges from 0.0271 mol min$^{-1}$ to 0.0358 mol min$^{-1}$, and the air feed rate is fixed at 0.129 mol min$^{-1}$. The corresponding equivalence ratios are 0.523–0.70, and the corresponding space velocities range from 28831 h$^{-1}$–31743 h$^{-1}$. Fig. 3 shows the heat supplies from the combustor to the water and the methanol evaporator versus $T_r$. It also illustrates the respective S/C ratios calculated by two different methods, $q_w/q_m$ (Eq. (4)) and the product analysis (Eq. (6)), respectively. The values from both methods agree well. The S/C ratios from $q_w/q_m$ are about 1.34 at 252 °C and 1.54 at 292 °C. With increasing $T_r$, the amount of $q_w$ increases faster than $q_m$. This is because a high heater temperature is more favorable to the vaporization of water, which has a higher boiling point and a larger heat of evaporation. Fig. 4 shows the composition of the product gas versus $T_r$. The results with methanol combustion will be discussed in Section 3.2. With hydrogen combustion, the concentration of $H_2$ remains near 74% on a dry basis with a slight increasing trend as $T_r$ is increased from 252 °C to 292 °C. The CO concentration increases remarkably with $T_r$ from 1.32% to 8.36%. The $CO_2$ concentration is highly correlated with the CO
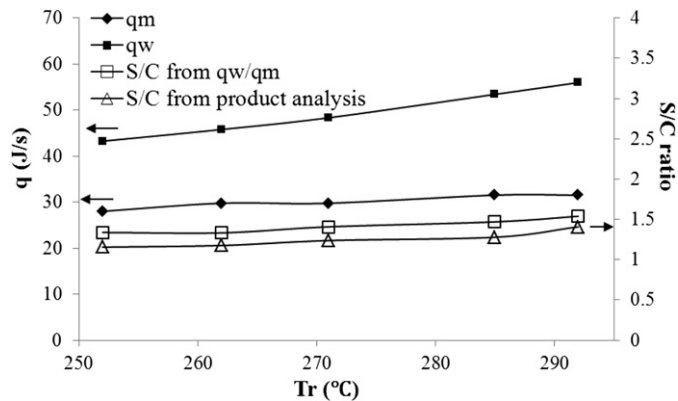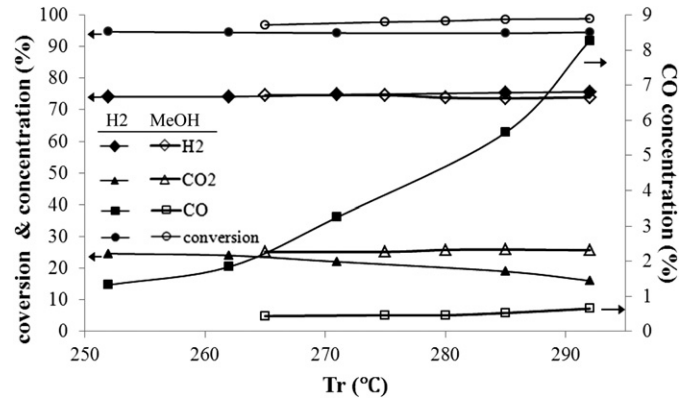


**Fig. 4.** Product composition versus reaction temperature with hydrogen or methanol combustion in the undiluted catalyst.

concentration, decreasing from 24.6% to 16.1%. Fig. 5 shows the corresponding temperature distributions measured by thermocouples T1–T7 with $T_r$ monitored at the center of the reformer. The respective positions of these thermocouples are shown in Fig. 2. Among T1–T7, T3 exhibits the highest temperatures because it is closest to the combustor inlet near which strong exothermic reaction is going. Away from the inlet region, T2 and T4–T6 exhibit lower temperatures. Interestingly, T5 shows the lowest temperatures except for the lowest $T_r$. This results from a combinative effect of the gradually decaying exothermic reaction in the u-turn-channel combustor and endothermic reaction in the serpentine-channel reformer. T5 is located near the turning section of the u-turn-channel combustor (cf. Fig. 2), where hydrogen combustion is significantly weaker after considerable consumption of hydrogen in the first channel section. This location also lies under the second channel of the serpentine-channel reformer (cf. Fig. 2), where the endothermic reforming reaction is still active. With weak heat release from the combustor and strong heat absorption from the reformer, T5 exhibits the lowest temperatures. At T6 and T7, which lies under the last section of the reformer channel, the temperatures are slightly higher due to the weak local endothermic reaction despite that the local heat release is even weaker than at T5. As shown in Fig. 5, the largest differences among T1–T7 are about 4–13 °C, increasing with $T_r$. In the next Section, we will show with detailed temperature measurements that the high CO concentrations shown in Fig. 4 result from high temperature non-uniformity.
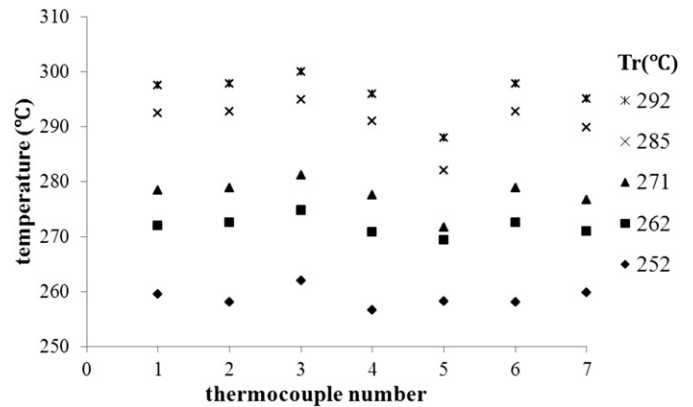


**Fig. 3.** The heat from hydrogen combustion to the water and the methanol evaporator versus reaction temperature.



**Fig. 5.** Temperature distributions within the reforming system at different reaction temperatures with hydrogen combustion in the undiluted catalyst.
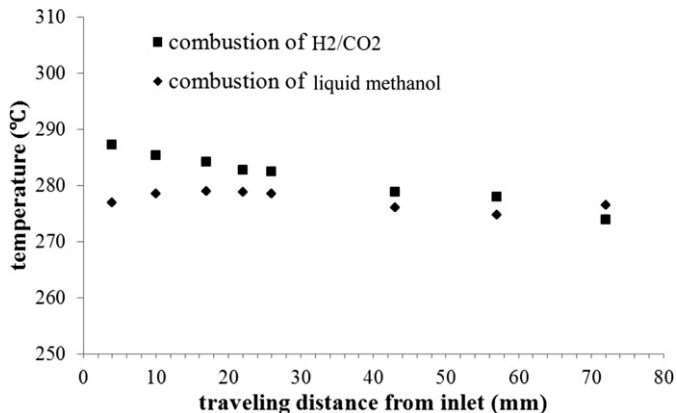
**Fig. 6.** Detailed temperature distributions versus traveling distance with combustion of hydrogen and methanol at $T_r = 275\ °C$ in the undiluted catalyst.

### 3.2. Differences with combustion of $H_2$ mixture and methanol in undiluted catalyst

To look into the detailed temperature distributions, we have added several thermocouples, besides T1 and T2, along the first section of the u-turn channel. The locations of these thermocouples are shown in Fig. 2. Then, we have retested by burning $H_2$ mixture and liquid methanol, respectively, both using the undiluted catalyst. Fig. 6 shows the detailed temperature distributions versus the traveling distance from the inlet respectively with combustion of $H_2$ mixture and methanol at $T_r = 275\ °C$. The first point, at a distance of 4 mm from the combustor inlet, exhibits the highest temperature with hydrogen combustion but a relatively low value with methanol combustion. Strong hydrogen combustion initiates from the inlet and the reaction gradually decays with continuous hydrogen consumption. In contrast, the liquid methanol is first vaporized after entrance, thereby showing lower temperatures in front of the active combustion slightly downstream. Fig. 7 shows the temperatures of T1–T7 with methanol combustion. As our previous results [14], the largest differences in these data are within 4 K. In general, the temperature distributions with methanol combustion are more uniform than those with hydrogen combustion. The methanol conversions and the product concentrations associated with different combustor fuels are compared in Fig. 4. With methanol combustion, the CO concentrations, lower than 0.64%, are superior to the high values with hydrogen combustion. In addition, the methanol conversions of 97%−98% are better than those of 94.5% with hydrogen combustion. In summary, the less
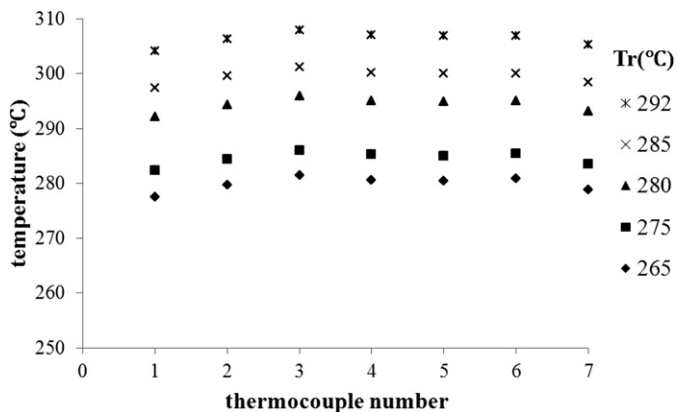
uniform temperature distributions with hydrogen combustion lead to not only greater CO concentrations but also lower methanol conversions.

### 3.3. MSR performance with combustion of $H_2$ mixture in diluted catalyst

To remedy the temperature non-uniformity with hydrogen combustion, we adopt the diluted catalyst formula to attenuate but elongate hydrogen combustion. Fig. 8 shows the improved



**Fig. 8.** Temperature distributions within the reforming system at different reaction temperatures with hydrogen combustion in the diluted catalyst.



**Fig. 9.** The methanol conversion and composition of the product gas versus reaction temperature with hydrogen combustion in the diluted catalyst.



**Fig. 7.** Temperature distributions within the reforming system at different reaction temperatures with methanol combustion in the undiluted catalyst.
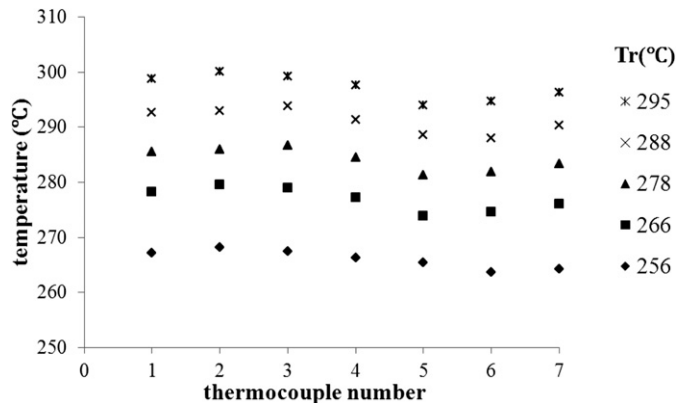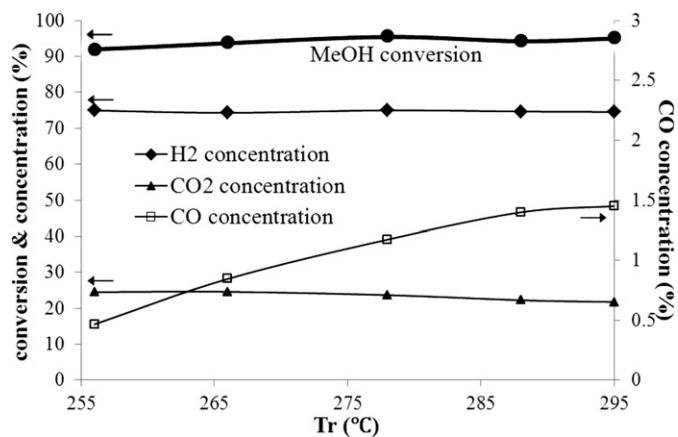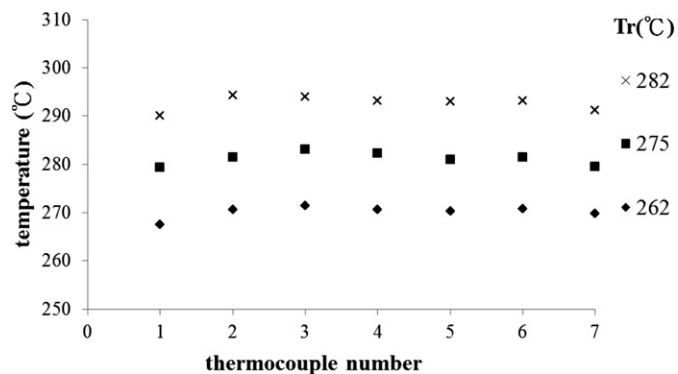


**Fig. 10.** Temperature distributions within the reforming system at different reaction temperatures with methanol combustion in the diluted catalyst.
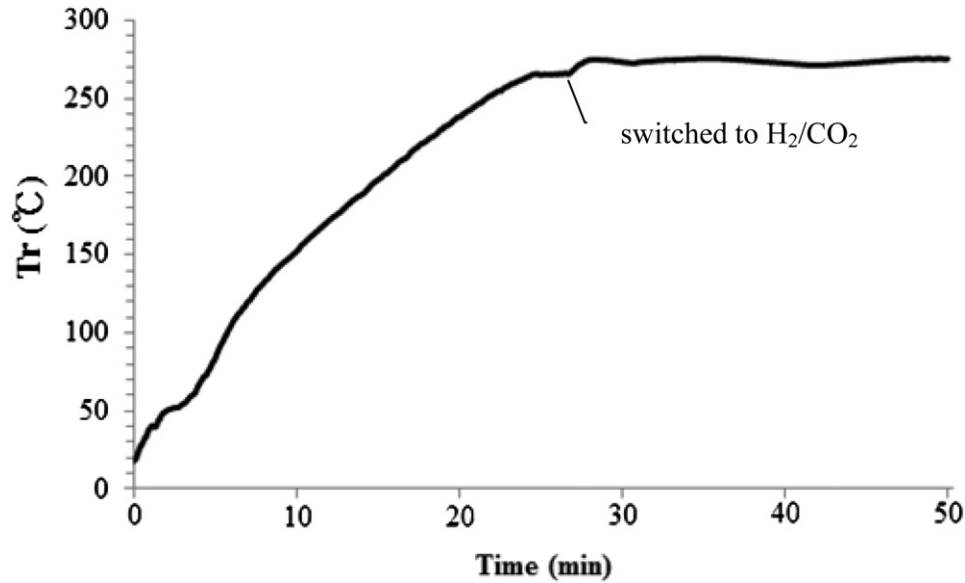
**Fig. 11.** The temperature history of a two-stage, bi-fueled process.

temperature distributions with hydrogen combustion in the diluted catalyst. Although T5 is still the lowest at most reaction temperatures, the maximum differences among T1–T7 are within 6 °C. This simple remedy effectively prolongs hydrogen reaction in the combustor and thereby improves the temperature uniformity. Fig. 9 shows the corresponding methanol conversions and compositions of the product gas versus $T_r$ when the $H_2$ mixture is burnt in the diluted catalyst. The methanol conversion increases from 92% at 256 °C to 95.2% at 295 °C. The CO concentration increases sensitively with $T_r$ from 0.47% to 1.45%. The $H_2$ concentration maintains at 74%–75%, and $CO_2$ decreases slightly with increasing CO. At 278 °C, there exists a highest methanol conversion of 95.6% with fairly low CO concentration of 1.17%. With the diluted catalyst, the reformer performance has also been tested using liquid methanol as the combustor fuel. Fig. 10 shows the corresponding temperature distributions in the reforming system. The temperature distributions resemble those adopting the undiluted catalyst (Fig. 7). However, using the diluted catalyst $T_r$ can only reach 282 °C by burning liquid methanol. The concentrations of $H_2$, $CO_2$ and CO at $T_r = 262$–282 °C are about 74%, 25% and 0.5%, respectively (not shown).

### 3.4. Two-stage bi-fueled process

A two-stage process has been conducted which begins with start-up by burning liquid methanol and is followed by combustion of exhaust hydrogen. The air feed rate is fixed at 0.129 mol min$^{-1}$. The $\dot{m}_{m,c}$ during the start-up is 0.013 mol min$^{-1}$, and the $\dot{m}_{h,c}$ afterwards is 0.032 mol min$^{-1}$. The history of the $T_r$ is illustrated in Fig. 11. It first needs 25 min for the reformer system to attain a steady state at $T_r = 270$ °C, similar to the 26 min in our previous experiment [14]. The CO concentration at this time is about 0.5% (not shown). After the combustor fuel was switched to exhaust hydrogen, the composition of the reformer product was analyzed every 5 min Fig. 12 shows the variations of methanol conversion and product composition versus time. Right after the switching, the CO concentration rapidly rises to 8.24% as a result of the unstable transition. It then gradually decreases to a stable value of 1.04% in 20 min. After the fuel switching, the $H_2$ concentration remains stably near 74% on a dry basis. The concentration of $CO_2$ increases slightly from 18.8% to 23.6% as the CO concentration decreases. The whole process needs about 45 min to attain a steady state at $T_r = 278$ °C, when the conversion increases to about 95% and the CO concentration decreases to 1.04%.
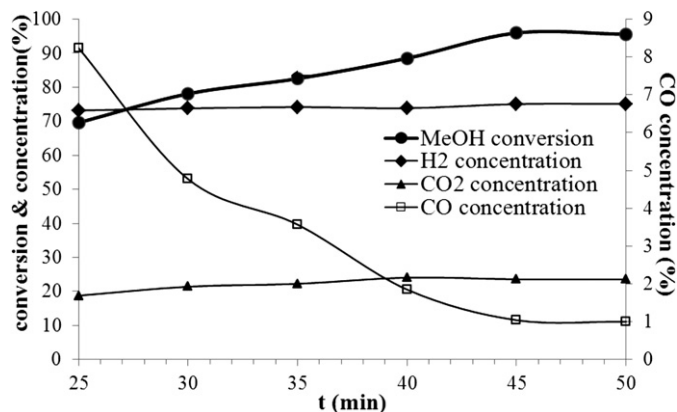
### 4. Conclusions

1. A novel passively-fed methanol steam reformer integrated with a u-turn-channel catalytic combustor fueled with either an $H_2/CO_2$ mixture or liquid methanol has been proven to yield high methanol conversions and low CO concentrations.
2. A suitably diluted catalyst formula can soothe the temperature non-uniformity with hydrogen combustion and retain the good uniformity with methanol combustion.
3. A two-stage process has been conducted to yield a high methanol conversion of 95% and acceptably low CO concentration of 1.04% under a steady state at a reaction temperature of 278 °C. It first takes 25 min to reach 270 °C by burning liquid methanol. After the combustor fuel is switched to the $H_2/CO_2$ mixture, another 20 min is needed to attain the steady state.



**Fig. 12.** The time variations of methanol conversion and product composition after fuel switching in the two-stage process.

## Acknowledgments

## References

[1] J.P. Breen, J.R.H. Ross, Catal. Today 51 (1999) 521–533.
[2] P.J. deWild, M.J.F.M. Verhaak, Catal. Today 60 (2000) 3–10.
[3] J. Agrell, H. Birgersson, M. Boutonnet, J. Power Sources 106 (2002) 249–257.
[4] J.D. Holladay, E.O. Jones, M. Phelps, J. Hu, J. Power Source 108 (2002) 21–27.
[5] B. Lindström, L.J. Pettersson, J. Power Sources 118 (2003) 71–78.
[6] P. Reuse, A. Renken, K. Haas-Santo, O. Gokre, K. Schubert, Chem. Eng. J. 101 (2004) 133–141.
[7] C. Liao, P.A. Erickson, Int. J. Hydrogen Energy 33 (2008) 1652–1660.
[8] E.A. Polman, J.M. Der Kinderen, F.M.A. Thuis, Catal. Today 47 (1999) 347–351.
[9] O.J. Kwon, D.H. Yoon, J.J. Kim, Chem. Eng. J. 140 (2008) 466–472.
[10] C.H. Leu, S.C. King, C.C. Chen, J.M. Huang, S.S. Tzeng, I.H. Liu, W.C. Chan, Appl. Catal. A: Gen. 382 (2010) 43–48.
[11] T. Kim, Int. J. Hydrogen Energy 34 (2009) 6790–6798.
[12] S.K. Ryi, J.S. Park, S.H. Choi, S.H. Cho, S.H. Kim, Chem. Eng. J. 113 (2005) 47–53.
[13] T. Kim, S. Kwon, Sen. Actuators A 154 (2009) 204–211.
[14] K.F. Lo, S.C. Wong, Int. J. Hydrogen Energy 36 (2011) 10719–10726.
[15] Y. Cao, Z. Guo, J. Power Sources 109 (2002) 287–293.
[16] E.R. Delsman, C.U. Uju, M.H.J.M. de Croon, J.C. Schouten, K.J. Ptasinski, Energy 31 (2006) 3300–3309.
[17] M.T. Janicke, H. Kestenbaum, U. Hagendorf, F. Schűth, M. Fichtner, K. Schubert, J. Catal. 191 (2000) 282–293.
[18] K.F. Lo, S.C. Wong, Int. J. Hydrogen Energy 36 (2011) 7500–7504.